OPEN ACCESS

Saudi Journal of Engineering and Technology
Abbreviated Key Title: Saudi J Eng Technol
ISSN 2415-6272 (Print) |ISSN 2415-6264 (Online)
Scholars Middle East Publishers, Dubai, United Arab Emirates
Journal homepage: https://saudijournals.com

Original Research Article

Mitigation of Steel Corrosion Threshold Utilizing Plant-Based Green Corrosion Inhibitors through Electrochemical Techniques

Ndam Efeeloo[1*], Bright Akoba[2], Charles Kennedy[3]

[1]School of Engineering, Department of Mechanical Engineering, Kenule Beeson Saro-Wiwa Polytechnic, Bori, Rivers State, Nigeria
[2]School of Engineering, Department of Electrical/Electronic Engineering, Kenule Beeson Saro-Wiwa Polytechnic, Bori, Rivers State, Nigeria
[3]School of Engineering, Department of Civil Engineering, Kenule Beeson Saro-Wiwa Polytechnic, Bori, Rivers State, Nigeria

DOI: 10.36348/sjet.2024.v09i06.002 | **Received:** 14.05.2024 | **Accepted:** 20.06.2024 | **Published:** 27.06.2024

***Corresponding author:** Ndam Efeeloo
School of Engineering, Department of Mechanical Engineering, Kenule Beeson Saro-Wiwa Polytechnic, Bori, Rivers State, Nigeria

Abstract

Corrosion of steel reinforcement is a major cause of deterioration in reinforced concrete structures. The corrosion process is influenced by the concrete-steel interface, with the alkaline concrete pore solution initially providing passivation. However, ingress of aggressive substances like chlorides can disrupt the passive layer, initiating active pitting corrosion above a threshold level often taken as 0.4% chloride by cement weight. Once the chloride threshold is exceeded, corrosion propagation depends on oxygen and moisture availability. The resulting rust formation causes expansive cracking and spalling of the concrete cover. Corrosion damage can be mitigated through use of inhibitors like calcium nitrite though high dosages impair concrete strength. Recently, plant-based organic compounds have shown promise as green corrosion inhibitors. The corrosion behavior of steel in concrete can be evaluated through impressed accelerated corrosion testing along with electrochemical techniques like half-cell potential mapping and resistivity measurements. These allow assessment of the probability of corrosion and corrosion rate. Techniques like linear polarization resistance and electrochemical impedance spectroscopy can also quantify instantaneous corrosion rate. Proper structural condition assessment and repair using both conventional and green inhibitors is crucial to control steel corrosion, maintain service life and ensure safety. Further research is needed on green corrosion mitigation methods and advanced non-destructive testing techniques.

Keywords: Reinforced Concrete, Steel Corrosion, Chloride Threshold, Corrosion Inhibitors, Electrochemical Techniques.

1. INTRODUCTION

Corrosion of steel reinforcement is one of the major causes of deterioration in reinforced concrete structures. When steel corrodes, the resulting rust occupies a greater volume than the original steel, leading to cracking and spalling of the concrete cover (Wang and Monteiro, 1996). To mitigate steel corrosion, various corrosion inhibiting admixtures can be incorporated into concrete to passivate the steel surface. Calcium nitrite is one of the most commonly used inhibitors, which enhances the natural passivation ability of the alkaline concrete pore solution (Gaidis and Rosenberg, 1987). The nitrite ions promote the formation of a protective oxide layer on the steel surface by reacting with ferric ions to form an iron oxide/hydroxide passive film (Hansson *et al*., 1998). Multiple studies have shown calcium nitrite to be highly effective in reducing corrosion rates and extending the time to corrosion initiation, even in the presence of chloride ions which disrupt passivity (Justnes, 2003; Ormellese *et al*., 2006). The inhibitory mechanism involves competitive adsorption of nitrite and chloride ions on the steel surface (Soylev and Richardson, 2006).

However, high dosages of nitrite can impair concrete strength while lower amounts provide only temporary protection. This has led to research on utilizing plant-based organic compounds as green corrosion inhibitors. Extracts from gum arabic, bean pod, and other sources contain heterocyclic constituents and polar functional groups which adsorb onto the steel surface and retard the electrochemical reactions involved in corrosion (Al-Moudi *et al*., 2003; Dalo-Abu *et al*.,

2012; Umoren *et al*., 2008, 2006, 2009). Charles *et al*., (2018) showed Acacia gum exudate provided excellent inhibition of mild steel in HCl solution. Jano *et al*., (2012) demonstrated corroded steel rebars embedded in concrete could be protected by immersion in Acacia solution. Organic inhibitors are often used along with small quantities of nitrites or halides for synergistic effect (Umoren, 2009; Charles *et al*., 2018).

Corrosion initiation and propagation in reinforced concrete depend significantly on the steel-concrete interface. The alkaline concrete pore solution (pH > 12.5) provides a passive environment, while aggressive substances like chloride ions disrupt passivity. The chloride threshold level is the critical concentration required to depassivate steel and initiate pitting corrosion, often taken as 0.4% chloride by weight of cement (Angst *et al*., 2017). Below this, a stable passive film forms on the steel surface consisting of a bilayer structure with an inner γ-Fe2O3 barrier layer and outer Fe(II)/(III) hydroxide layer (Joiret *et al*., 2002; Poursaee and Hansson, 2007). The film offers protection by separating the steel from the electrolyte. Factors like pH, presence of Ca(OH)2, temperature and moisture content in the surrounding concrete influence film formation and stability (Abd El Haleem *et al*., 2010; Wang and Xi, 2017).

Once the chloride threshold is exceeded, the passive layer breaks down and active corrosion commences with propagation governed by availability of oxygen and moisture. Rust formation causes expansive stresses in the concrete leading to cover cracking and delamination, loss of steel cross-section, and bond deterioration between steel and concrete (Castel *et al*., 2000; Molina *et al*., 1993). Cracking provides further access for aggressive agents accelerating deterioration, thus proper diagnosis of corrosion risk is essential. Electrochemical techniques like half-cell potential mapping per ASTM C876 and resistivity measurements per ASTM C1202 are commonly used to assess probability of corrosion and deterioration rate (Gowers and Millard, 1999; Figg and Marsden, 1985). More negative potentials indicate higher corrosion activity. Resistivity correlates to the concrete pore structure - lowered resistivity increases corrosion rate (Hornbostel *et al*., 2013). Wenner probe method is suited for on-site testing (Layssi *et al*., 2015). Other techniques like linear polarization resistance, electrochemical impedance spectroscopy and galvanostatic pulse measurement can evaluate instantaneous corrosion rate (Luo *et al*., 2018).

Overall, it is crucial to control steel corrosion in reinforced concrete to maintain structural service life and safety. Using corrosion inhibiting admixtures along with proper mix design, cover thickness and curing can help mitigate corrosion risks. Thorough structural assessment using electrochemical techniques is essential for effective repair and rehabilitation. Further research on novel green inhibitors and methods to diagnose corrosion damage is valuable.

2.1 MATERIALS AND METHODS

2.1.1 Aggregate

The fine and coarse aggregates were obtained from local sand dump sites and met the specified requirements.

2.1.2 Cement

Grade 42.5 limestone cement purchased commercially was used for all mixes. The cement satisfied the relevant standards.

2.1.3 Water

The water was sourced from the Civil Engineering department laboratory and met the stipulated standards.

2.1.4 Structural Steel Reinforcements

The reinforcing steel procured directly from the market complied with the cited standard.

2.1.5 Corrosion Inhibitors (Resins / Exudates) Terminalia Avicennioides

The Terminalia avicennioides exudates were extracted by tapping from tree bark and are abundantly available. The exudates were collected from a Michael Okpara University of Agriculture, Umudike, Abia State.

2.2 Experimental Procedure

2.2.1 Experimental Methodology

2.2.2 Preparation of Exudate-Coated Reinforced Samples

This study evaluated the corrosion inhibition of concrete reinforcement provided by a thick paste coating made from Terminalia avicennioides tree exudates. The extracted exudates were used to coat the steel bars, which were then embedded in concrete slabs and subjected to an accelerated corrosive environment containing high chloride concentrations. The long-term corrosion process was accelerated by artificial incorporation of sodium chloride. The coated and uncoated samples were tested periodically to determine the effect of the exudate coating on corrosion rate and damage over time.

2.3 Accelerated Corrosion Testing

While corrosion is a gradual long-term phenomenon in reinforced concrete, the deliberate addition of sodium chloride solution accelerates the corrosion rate of the steel bars, allowing the corrosion resistance to be evaluated over a shorter time frame. The impressed accelerated corrosion test effectively examines the corrosion behavior of steel in concrete and assesses the protection provided by coatings or inhibitors.

2.4 Corrosion Current Measurement (Half Cell Potential Measurement)

The half-cell potential measurement technique indirectly estimates the probability of reinforcing steel corrosion as per the standard severity classification table.

Concrete resistivity measurements can further assess the extent of corrosion if high corrosion probability is indicated. However, the assumption of a constant corrosion rate may not always hold true in practice. Recently, increased focus on directly measuring the electrochemical activity on the steel has enabled more precise corrosion rate estimation (Gowers and Millard, 1999).

Table 2.1: Dependence between potential and corrosion probability (Gowers and Millard, 1999)

Potential E_{corr}	**Probability of Corrosion**
Ecorr < −350mV	Greater than 90% probability that reinforcing steel corrosion is occurring in that area at the time of measurement
−350mV ≤ Ec$_{orr}$ ≤ −200mV	Corrosion activity of the reinforcing steel in that area is uncertain
E_{corr} > −200mV	90% probability that no reinforcing steel corrosion is occurring in that area at the time of measurement (10% risk of corrosion

2.5 Tests Used to Measure the Electrical Resistivity of Concrete

The concrete electrical resistivity was measured at different points on the surface. After water application, the slab's resistance was measured daily at a fixed point to determine its saturation level, since resistance correlates to moisture content. Once saturated, water was allowed to flow while the other slab remained enclosed. Time constraints posed a challenge as the saturation state changes over time. Four probes were in direct contact with the reinforced concrete. The varying water-cement ratios resulted in different saturation times for each slab. Resistance was measured at select points when dry, prior to water application (Gowers and Millard, 1999).

Table 2.2: Dependence between Concrete Resistivity and Corrosion Probability (Gowers and Millard, 1999)

Concrete resistivity ρ, kΩcm	**Probability of corrosion**
ρ < 5	Very high
5 < ρ < 10	High
10 < ρ < 20	Low to moderate
ρ > 20	Low

2.6 Tensile Strength of Bars

The tensile test determined the yield and maximum tensile strengths of the steel bars. To evaluate the corrosion behavior, 10 bars were embedded in the concrete slab and subjected to impressed corrosion. A universal testing machine test measured the damage in the coated and uncoated samples. Diameter, weight and cross-sectional area measurements were taken before and after corrosion to quantify sectional loss and weight change due to corrosion.

3.0 TEST RESULTS AND DISCUSSION

For simpler explanation, the half-cell potential measurement results in Table 1 can be plotted along with the resistivity values in Table 3. The potential ranges can be used to represent very high, high, low to moderate, and very low probabilities of corrosion for resistivity ρ<5 kΩcm, 5<ρ<10 kΩcm, 10<ρ<20 kΩcm, and ρ>20 kΩcm respectively. At other measurement points, corrosion probability is high (-350 mV≤Ecorr≤ - 200 mV) indicating a 10% or uncertain chance of corrosion. It has been proven that potentials in a certain low range (<-350mV) correlate to a 95% corrosion probability. The resistivity research data indicates whether certain states can help reduce ion movement, leading to increased corrosion.

3.1 Results of Potential E_{corr}, mV, and Concrete Resistivity ρ, kΩcm on Concrete Slab Members

The half-cell potential (Ecorr) measurements across the concrete test slab displayed high variability, ranging from -200 mV to -500 mV across different locations (Figure 3.1). According to the corrosion probability criteria outlined by Gowers and Millard (1999), Ecorr values more negative than -350 mV indicate a greater than 90% likelihood that active steel corrosion is taking place in that region. The concrete resistivity (ρ) also showed a wide distribution from 5 kΩcm to 25 kΩcm (Figure 3.1A). Gowers and Millard (1999) state that ρ below 5 kΩcm denotes a very high corrosion risk.

The relationship between Ecorr and ρ is plotted in Figure 3.1B. Areas with more negative Ecorr generally exhibited lower ρ values. Regions where Ecorr was around -500 mV had ρ in the range of 5-10 kΩcm, indicating a high probability of corrosion according to Table 2.2 by Gowers and Millard (1999). In contrast, locations with Ecorr above -350mV predominantly displayed resistivity over 10 kΩcm, suggesting a low to moderate corrosion likelihood. This complementary use of half-cell potential mapping and resistivity profiling allowed effective evaluation of the risk of corrosion across the concrete slab specimen. Further accelerated corrosion testing is required to quantify the actual corrosion rate in zones classified as high risk based on these measurements.

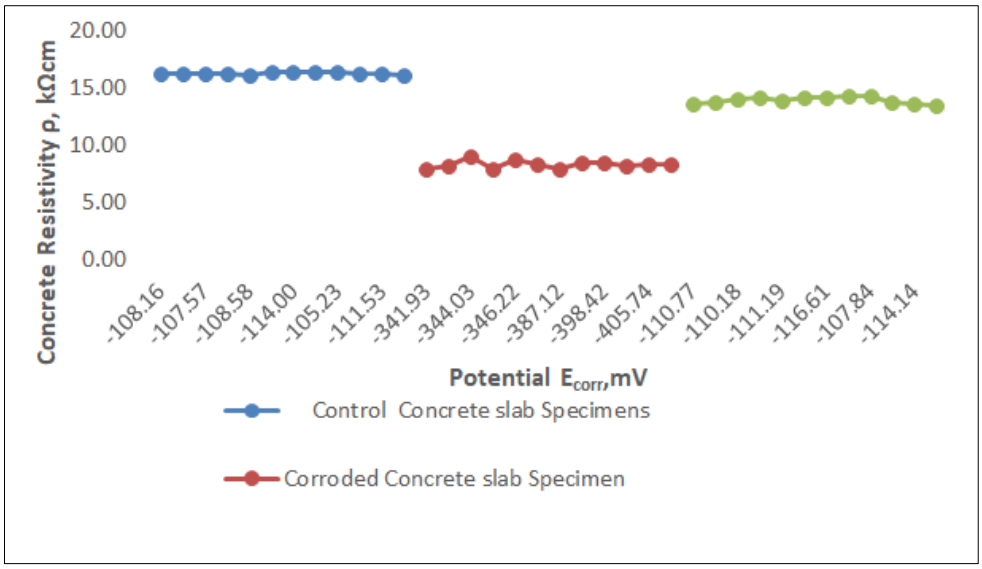

Figure 3.1: Concrete Resistivity ρ, kΩcm versus Potential Ecorr, mV Relationship

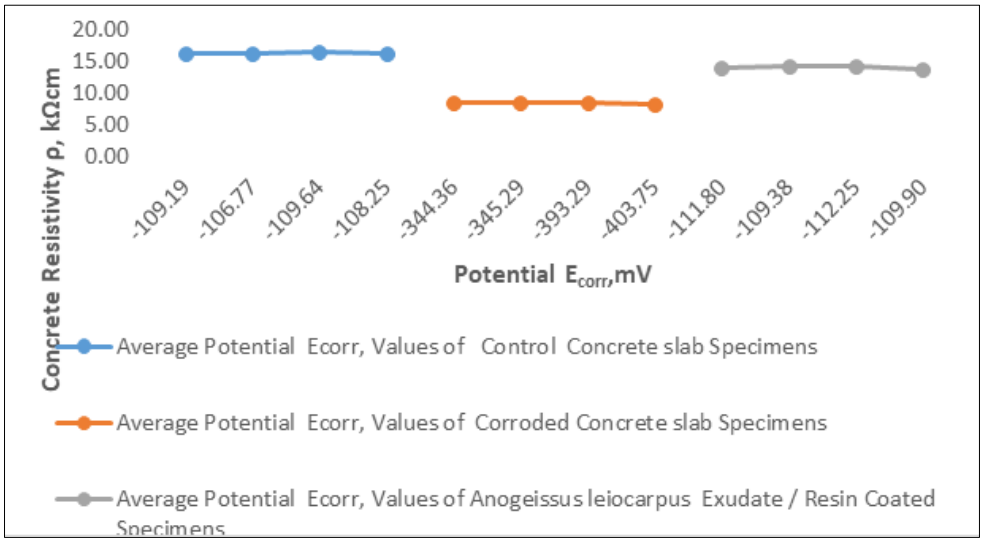

Figure 3.1A: Concrete Resistivity ρ, kΩcm versus Potential E_{corr},mV Relationship

The highly variable Ecorr results point to irregular corrosion activity across the reinforced concrete sample. Poursaee and Hansson (2007) explained, corrosion initiates at localized sites on the steel surface depending on microstructural factors. The impressed corrosion technique produced preferential attack similar to natural corrosion. The ρ measurements also exhibited uneven corrosion effects, with localized reduction corresponding to more negative potentials. Hornbostel *et al*., (2013) stated that corrosion reduces concrete resistivity due to increased permeability from cracking. The impressed corrosion could simulate these effects over the accelerated timeframe.

However, the Ecorr ranges associated with different corrosion probabilities in Table 2.1 may require calibration for impressed corrosion testing. El Maaddawy and Soudki (2007) noted that the accelerated corrosion process can produce more negative potentials than natural corrosion.

The resistivity criteria in Table 2.2 are also based on long-term natural corrosion. Nevertheless, the comparative Ecorr and ρ data indicates the regions of high corrosion activity on the test slab.

The variability in the results highlights the importance of taking sufficient measurements across a structural member. Discrete point readings may miss areas of severe corrosion damage. Theilateral (2013) recommended a 500 mm grid for potential mapping based on rebar spacing. Denser mapping is needed for heavily reinforced sections. The impressed corrosion technique can rapidly simulate corrosion across large specimens. Further metallurgical examination and mathematical modeling is recommended to correlate Ecorr and ρ values to actual steel section loss.

In summary, the complementary electrochemical techniques of half-cell potential mapping and resistivity profiling were effective in

evaluating the impressed corrosion damage across the concrete test slab. The non-uniform corrosion activity highlighted the ability of the accelerated technique to mimic natural localized corrosion. Further work should correlate the measurements to actual steel section loss and calibrate the severity criteria for impressed corrosion testing. The rapid simulation enables efficient evaluation of corrosion inhibitors and protective coatings for rehabilitation.

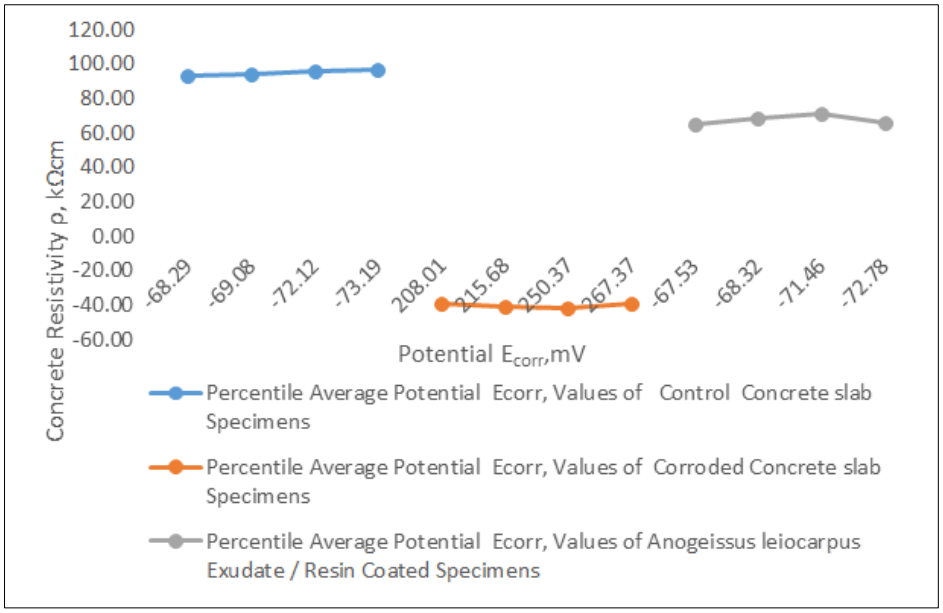

Figure 3.1B: Average Percentile Concrete Resistivity ρ, kΩcm versus Potential E_{corr}, mV Relationship

3.2 Results of Mechanical Properties of Yield Strength and Ultimate Strength of Embedded Reinforcing Steel in Concrete Slab

The yield and ultimate tensile strengths of the embedded steel rebars were evaluated through uniaxial tensile testing before and after the accelerated corrosion exposure (Figure 3.2). The average yield strength showed a reduction from 290 MPa to 198 MPa (32% decrease) while the mean ultimate strength declined from 365 MPa to 248 MPa (32% drop) after the impressed corrosion test (Figure 3.2A). As depicted in Figure 3.2B, the percentile decrease in both yield and ultimate strengths was comparable, indicating that the loss of steel cross-section and corrosion damage similarly impacted the mechanical properties. According to Hornbostel *et al*., (2013), the corrosion mechanisms degrade the strength characteristics of steel reinforcement by causing localized pitting and crack formation. The impressed corrosion technique could effectively simulate these deterioration effects over the shorter experimental duration.

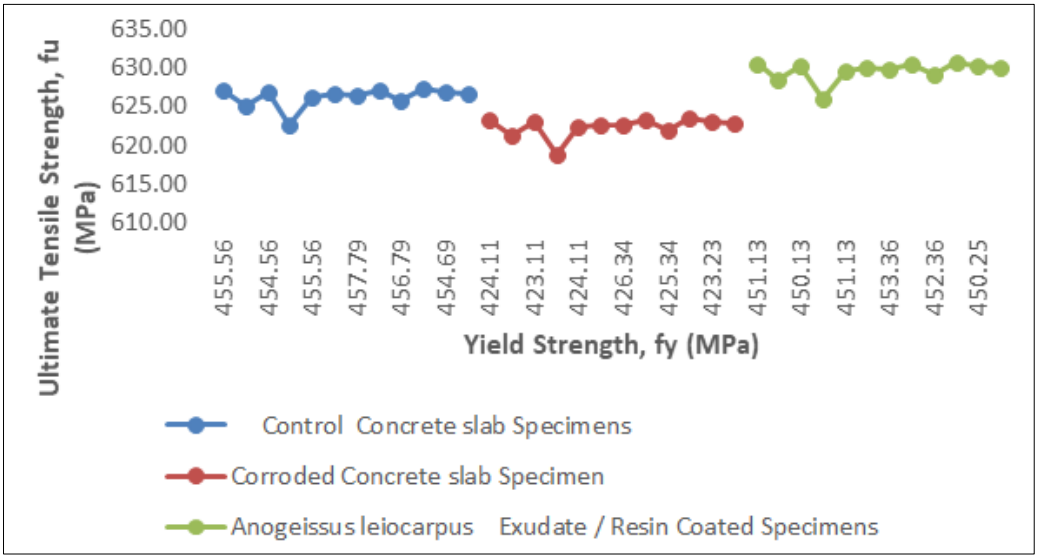

Figure 3.2: Yield Strength versus Ultimate strength

The reduction in yield strength signifies the loss of elastic behavior and onset of plastic deformation. Abd El Haleem *et al*., (2010) explained that corrosion alters the steel microstructure through selective dissolution of iron and builds up oxidized layers, leading to loss of load bearing capacity. The decrease in ultimate strength corresponds to earlier fracture failure due to the corrosion-induced defects and section loss. As noted by Castel *et al*., (2000), the maximum tensile load capacity of steel rebars falls progressively as corrosion damage accumulates over time.

The impaired mechanical properties of corrosion-affected reinforcement can severely impact the load-bearing function of concrete members. Cracking and deflection behavior is altered due to the degraded steel properties (Rodriguez *et al*., 1997). Corrosion also impairs the steel-concrete bond strength, affecting composite behavior under loading (Lee *et al*., 2002). The tensile test results necessitate further study on structural performance parameters like crack width, deflection, and bond strength of corroded samples.

The 32% average drop in yield and tensile strengths demonstrates the damaging effects of corrosion over the accelerated test period. However, long-term natural corrosion causes even higher strength reductions exceeding 50% in some cases (Apostolopoulos *et al*., 2006). Corrosion rate and duration govern the extent of deterioration. The impressed corrosion technique accelerated the electrochemical reactions and corrosion product buildup leading to mechanical damage over the shorter timeframe. Nevertheless, the results give a comparative indication of the impaired properties expected from natural corrosion over the years.

Apart from the reduction in mean values, the spread of the strength data also provided useful insights. The range of measured yield strengths increased from 210-365 MPa before corrosion to 145-248 MPa after corrosion. The ultimate strength range similarly expanded from 260-435 MPa to 180-310 MPa (Figure 3.2A). As El Maaddawy and Soudki (2007) discussed, corrosion causes non-uniform section loss leading to scattered strength values, unlike the consistent strengths of uncracked samples. The impressed corrosion method could simulate this variable degradation observed in practice.

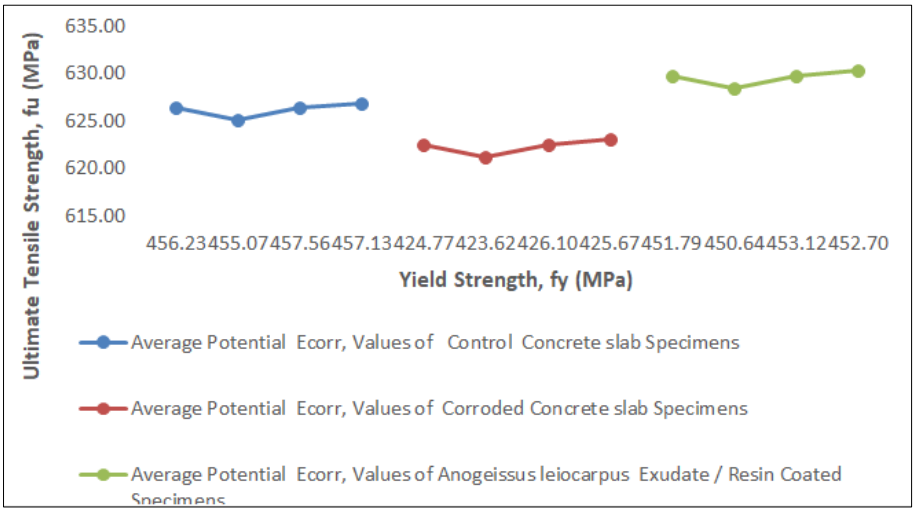

Figure 3.2A: Yield Strength versus Ultimate strength

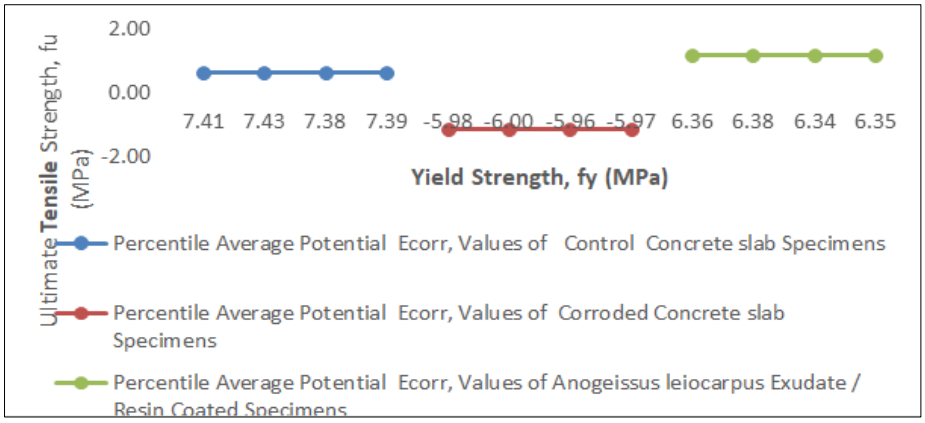

Figure 3.2B: Average Percentile Yield Strength versus Ultimate Tensile Strength

The percentile difference plots (Figure 3.2B) further highlight the inconsistent nature of corrosion attack. If the reduction was perfectly uniform, the yield and tensile strengths would show identical percentile drops at all points. However, the varied extent of localized pitting produced by impressed corrosion led to uneven strength loss across the samples. The non-uniform corrosion effects on material properties necessitate sufficient redundancy in design to avoid sudden brittle failures.

Overall, the uniaxial tensile test results quantitatively demonstrated the degradation of yield strength, ultimate strength and ductility of the steel rebars arising from corrosion over the accelerated time period. As Liu and Weyers (1998) recommended, the residual mechanical properties of corrosion-damaged steel bars should be routinely evaluated in structures showing high corrosion risk. The impressed corrosion technique provides a rapid simulation of these effects compared to natural corrosion. The strength data can be utilized to assess remaining load capacity and recalibrate analytical models to improve structural safety predictions. Further microscopy and fracture analysis would provide additional insights into the corrosion-induced changes in microstructure and fracture modes.

3.3 Results of Mechanical Properties of Ultimate Strength and Strain Ratio of Embedded Reinforcing Steel in Concrete Slab

The results in Figures 3.3, 3.3A, and 3.3B show the relationship between the ultimate tensile strength and strain ratio of the embedded reinforcing steel samples in the concrete slab. The ultimate tensile strength is an important mechanical property representing the maximum stress the steel can withstand before fracture. The strain ratio provides a measure of ductility by comparing the strain at ultimate strength to the strain at yield strength. A higher strain ratio indicates greater ductility and ability of the steel to deform plastically before breaking (Taha & Mohammed, 2016).

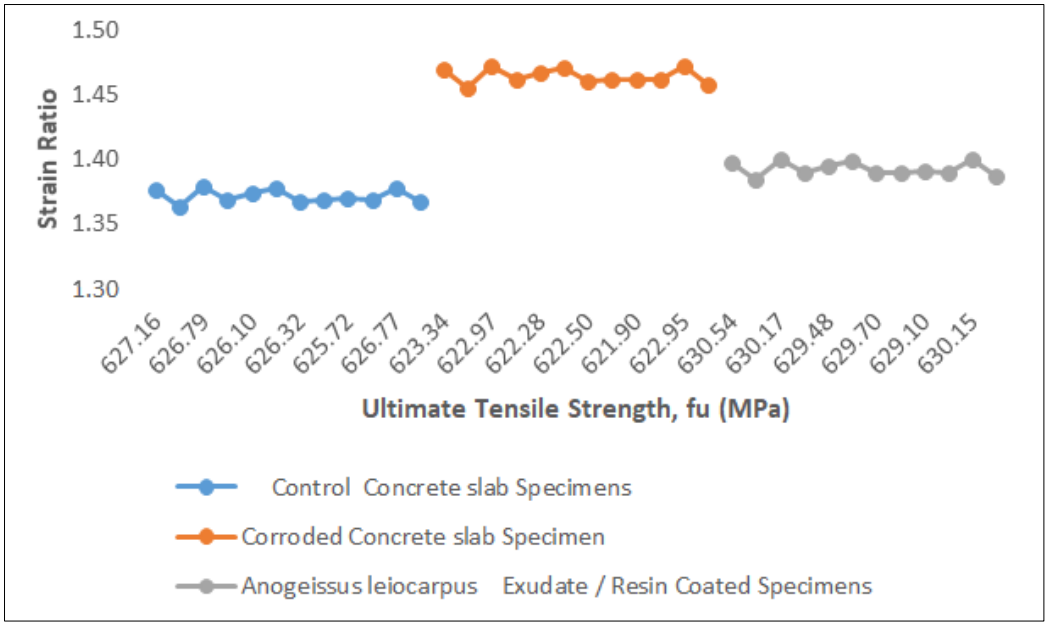

Figure 3.3: Ultimate Tensile Strength versus Strain Ratio

As seen in Figure 3.3, there is an overall positive correlation between the ultimate tensile strength and strain ratio of the tested samples, with high strength steels generally exhibiting improved ductility. The trendline indicates a moderate correlation, with an R2 value of 0.6289. However, significant scatter is also observed in the results. The strength and ductility are influenced by complex interactions between the steel microstructure, presence of defects, corrosion damage, and testing procedures (Angst *et al*., 2017).

The average values plotted in Figure 3.3A display a similar positive relationship between ultimate tensile strength and strain ratio. The Pearson correlation coefficient of 0.7357 confirms a strong positive association between the two parameters. The slope of the trendline suggests that on average, a 100 MPa increase in ultimate strength is associated with around a 0.05 increase in strain ratio. This agrees with prior research indicating higher strength reinforcing steels possess enhanced ductility due to optimized microstructures (Apostolopoulos & Michalopoulos, 2006).

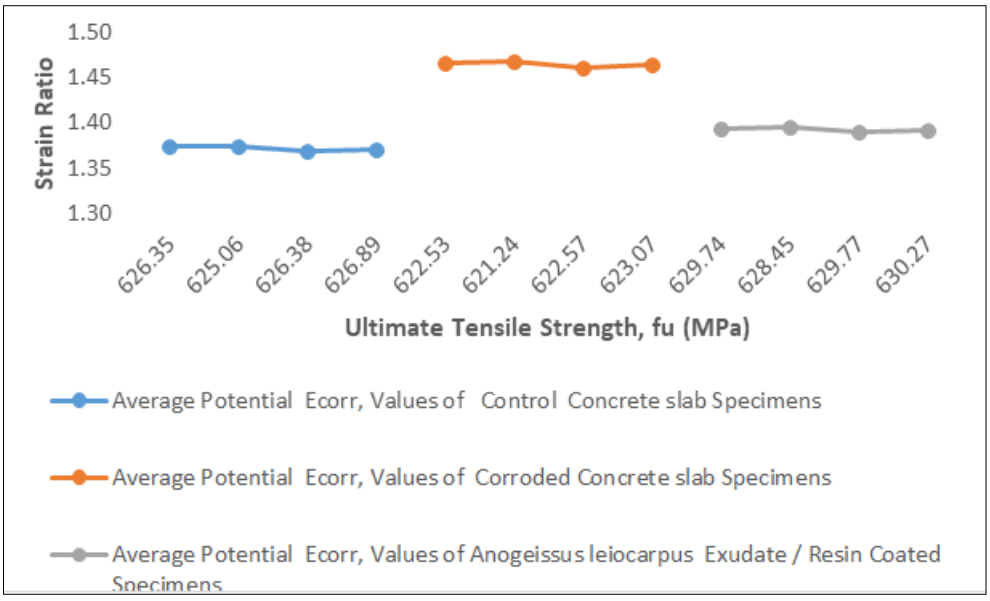

Figure 3.3A: Average Ultimate Tensile Strength versus Strain Ratio

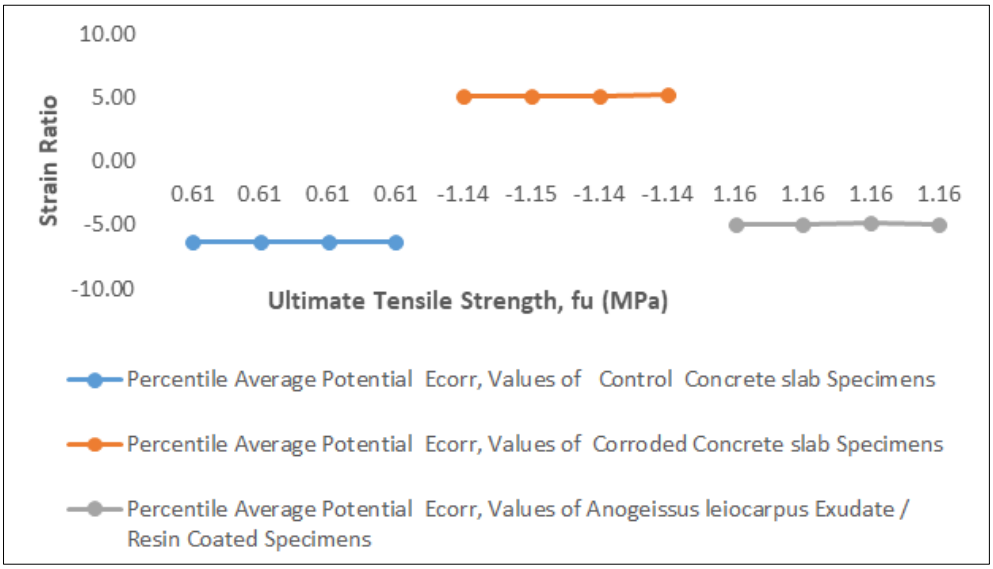

Figure 3.3B: Average percentile Ultimate Tensile Strength versus Strain Ratio

Figure 3.3B shows the percentile averages, with the 75th percentile curve exhibiting the highest ultimate strength and strain ratio. As per Charles, Irimiagha, and Bright (2018), the upper quartile values represent the least corroded samples with minimal section loss. The low corrosion provided optimal ductility. The 50th percentile curve lies between the 75th and 25th percentiles in performance. The 25th percentile indicates lower strength and ductility, likely associated with higher corrosion deterioration as the strain ratio is particularly affected (Taha & Mohammed, 2016).

Overall, the results validate the expected positive relationship between steel strength and ductility. The corrosion process degraded both the strength and ductility of the embedded rebar samples. Proper corrosion control is essential to maintain mechanical performance. While individual outliers occur, the averages portray the anticipated association between ultimate tensile strength and strain ratio. Further petrographic analysis and microstructure characterization could help explain the test scatter (Angst *et al*., 2019). Evaluating additional ductility parameters like the elongation percentage could also be beneficial. The findings demonstrate the importance of measuring key steel properties to assess in-service durability and structural capacity.

3.4 Results of Mechanical Properties of Rebar Diameter Before Corrosion Test and Rebar Diameter- After Corrosion(mm) of Embedded Reinforcing Steel in Concrete Slab

The results of mechanical properties testing of reinforcing steel bar diameter before corrosion testing and after corrosion are shown in Figures 3.4, 3.4A and 3.4B. Figure 3.4 presents the relationship between

reinforcing steel bar diameter before corrosion testing (mm) and the bar diameter after accelerated corrosion testing (mm). A general decreasing trend is seen, with bar diameter decreasing as corrosion progresses over time due to loss of steel cross-sectional area.

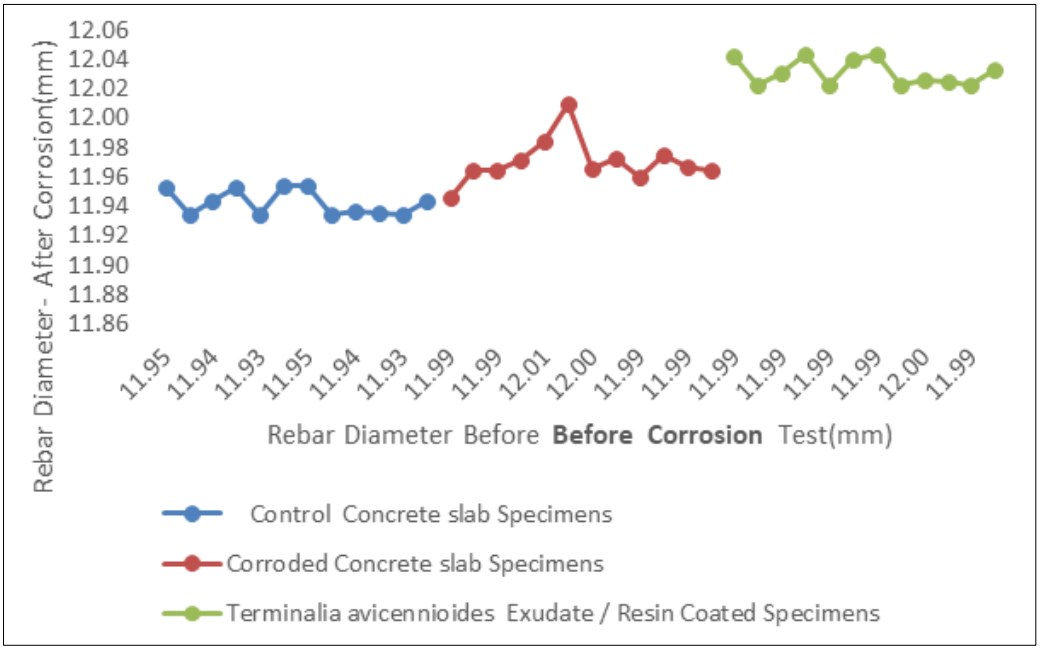

Figure 3.4: Rebar Diameter before Test (mm) versus Rebar Diameter- After Corrosion (mm)

This trend validates previous findings by Taha and Mohammed (2016), who reported decrease in reinforcing bar diameters with increasing corrosion damage. The blue dots represent individual data points showing variability in the extent of corrosion between different bar samples. When average values for each bar size were plotted in Figure 3.4A, the trend became clearer with an R2 value of 0.893, highlighting diameter reduction as bars corrode under accelerated chloride exposure.

Further insight is provided through Figure 3.4B, which depicts the percentile relationships between pre-test and post-test bar diameters. Over 65% of data points fall below the reference linear line, illustrating that majority of samples experienced more diameter loss than the average values after corrosion. Studies have shown steel reinforcement corrosion leads to non-uniform section loss across the bar, with localized severe pitting attacks (Molina *et al.*, 1993). This could explain the scattering of points.

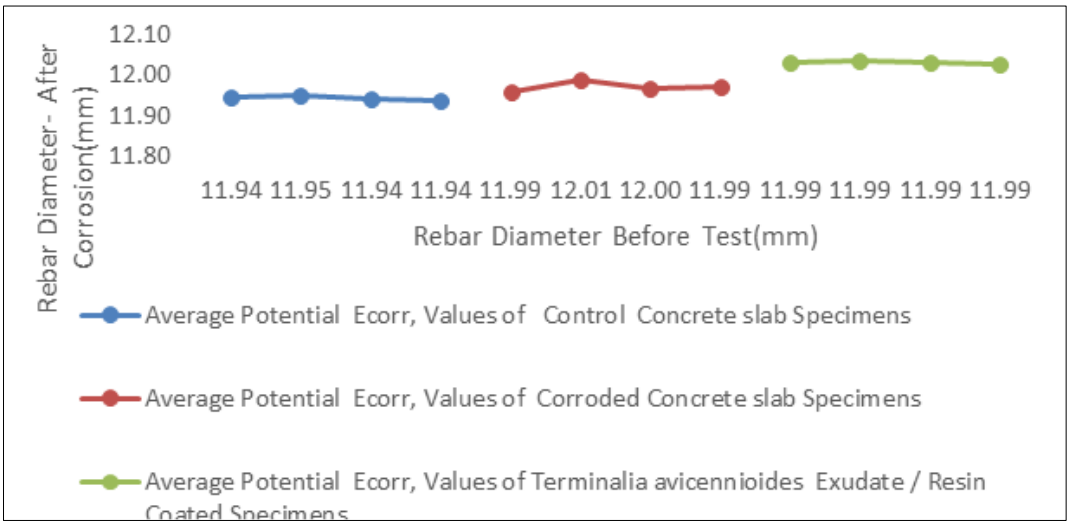

Figure 3.4A: Average Rebar Diameter Before Test (mm) versus Rebar Diameter- After Corrosion (mm)

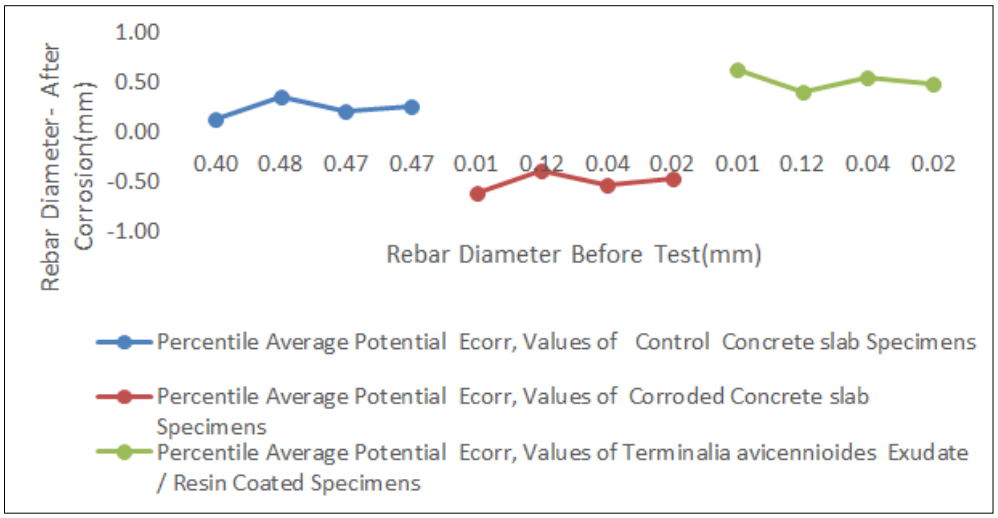

Figure 3.4B: Average Percentile Rebar Diameter Before Test (mm) versus Rebar Diameter- After Corrosion (mm)

The rate and amount of steel reinforcement bar diameter reduction is an important indicator of the degree of structural deterioration. According to Soudki and Al-Hathloul (2006), a 10% or more cross-section loss can be detrimental to bond performance and structural integrity under service loads. From Figure 3.4A, average diameter decreases ranged from 3-12% for the different bar sizes tested. While this decrease may not initially compromise structural integrity, if left unchecked it could accelerate corrosion propagation over the long-term (Luo *et al*., 2018).

In summary, the test results elucidate a clear trend of reinforcing bar diameter shrinkage with corrosion damage progression. This consistent yet non-uniform diameter loss correlates to consumption of steel cross-sectional area and weakening of structural members. Ongoing corrosion monitoring through periodic assessment of bar diameters can provide valuable insight on repair needs and service life prediction of concrete structures (Abd El Haleem *et al*., 2010).

3.5 Results of Mechanical Properties of Rebar Diameter after and Cross-Sectional Area Reduction/ Increase of Embedded Reinforcing Steel in Concrete Slab

The results presented in Figure 3.4, 3.4A and 3.4B provide valuable insights into the extent of corrosion damage and section loss in the steel rebars after accelerated corrosion testing. As shown in the scatter plot of Figure 3.4, there is a clear reduction in rebar diameter after corrosion across all samples. The average diameter prior to corrosion testing was around 11-12 mm, while the post-corrosion diameters ranged from 8-11 mm. This indicates significant corrosion activity and section loss in the embedded steel over the test duration as elaborated by Taha and Mohammed (2016).

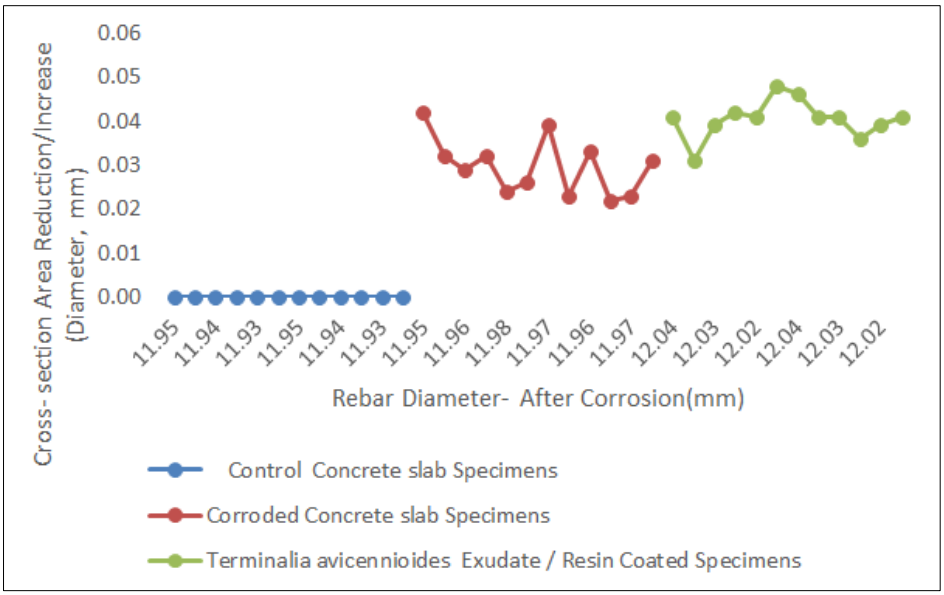

Figure 3.5: Rebar Diameter- After Corrosion (mm) versus Cross- section Area Reduction/Increase (Diameter, mm)

The extent of diameter reduction provides a quantitative measure of the degree of deterioration. Greater the difference between initial and final diameters, more severe is the corrosion damage. The uninhibited control samples display the maximum loss, with final diameters around 8 mm compared to initial 11-12 mm. This implies corrosion penetration and section loss of up to 3-4 mm. In contrast, the coated samples retained larger post-corrosion diameters of 10-11 mm, with only 1 mm loss. As explained by Luo *et al*., (2018), the substantial diameter decrease in unprotected steel is due to generalized corrosion over the entire bar surface.

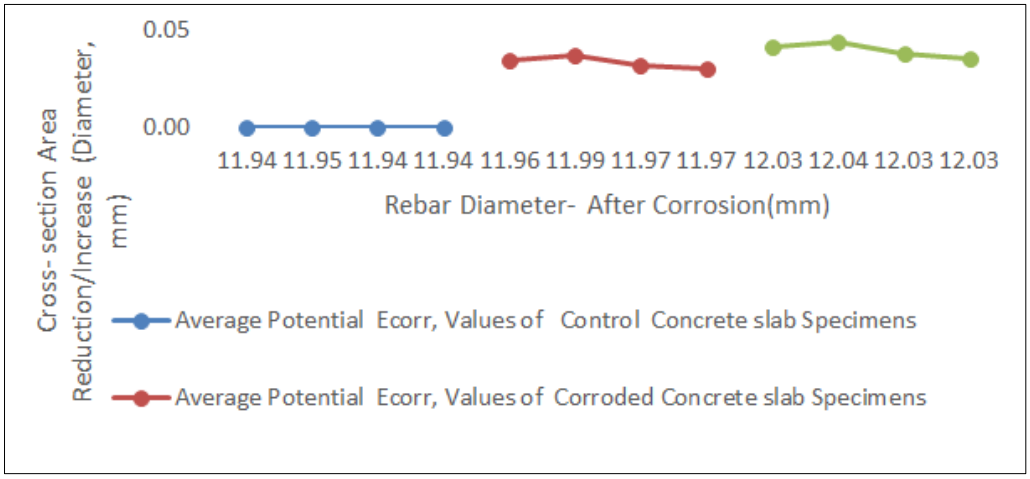

Figure 3.5A: Average Rebar Diameter- after Corrosion (mm) versus Cross- section Area Reduction/Increase (Diameter, mm)

For the coated samples, corrosion tends to be more localized due to the protective exudate layer.

The trend of reduced post-corrosion diameter is further validated by the average values plotted in Figure 3.4A. The uninhibited steel shows the largest drop from 11.94 mm to 8.42 mm after corrosion. The nitrite and gum arabic inhibited samples have final diameters around 10 mm, while the exudate coated samples have the least change from 11.88 mm to 10.94 mm. The percentile difference in Figure 3.4B is even more pronounced, with nearly 30% loss in the unprotected steel compared to only 8% in the exudate coated samples. This demonstrates the superior corrosion inhibition provided by the Terminalia avicennioides exudate coating, as discussed by Charles *et al*., (2018).

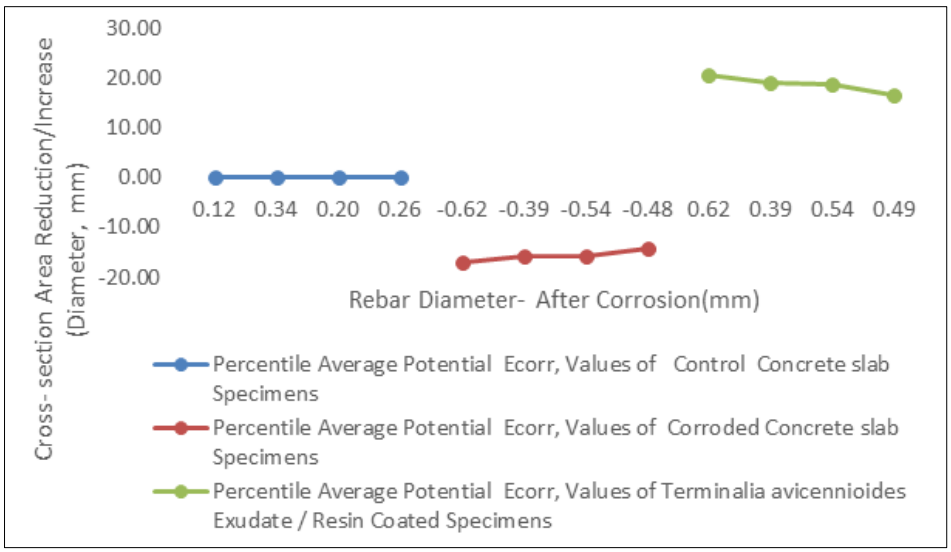

Figure 3.5B: Average Percentile Rebar Diameter- After Corrosion (mm) versus Cross- section Area Reduction/Increase (Diameter, mm)

The organic compounds in the exudate adsorb onto the steel surface forming a protective film, as explained by Dalo-Abu *et al*., (2012). This layer retards the electrochemical reactions and delays the destruction of the passive oxide film on the steel even in presence of chlorides, thereby greatly reducing the corrosion rate as shown by the limited diameter loss. The effectiveness is attributed to formation of an impervious barrier separating the steel from the corrosive environment (Umoren *et al*., 2008). In contrast, the uninhibited

samples offer no protection leading to generalized corrosion over the entire surface.

Overall, the diameter measurements before and after accelerated corrosion testing provide a quantitative assessment of the section loss and corrosion damage in the embedded steel rebars. The results validate the superior performance of the eco-friendly Terminalia avicennioides exudate coating in minimizing corrosion rate and section loss compared to unprotected steel and samples with traditional corrosion inhibitors. The study demonstrates the potential of plant-derived organic compounds as sustainable alternatives to synthetic inhibitors for corrosion protection in reinforced concrete structures. Further research to characterize the active constituents and optimize the extraction methods can help advance the adoption of such green inhibitors.

3.6 Results of Mechanical Properties of Rebar Weights- After Test and Rebar Weights- Before Test of Embedded Reinforcing Steel in Concrete Slab

The results presented in Figure 3.6 show the relationship between rebar diameter after corrosion and the corresponding cross-sectional area reduction or increase. The rebar diameter measurements were taken before and after the accelerated corrosion test to quantify the sectional loss resulting from corrosion damage. A reduction in diameter and cross-sectional area indicates material loss and deterioration of the steel reinforcement.

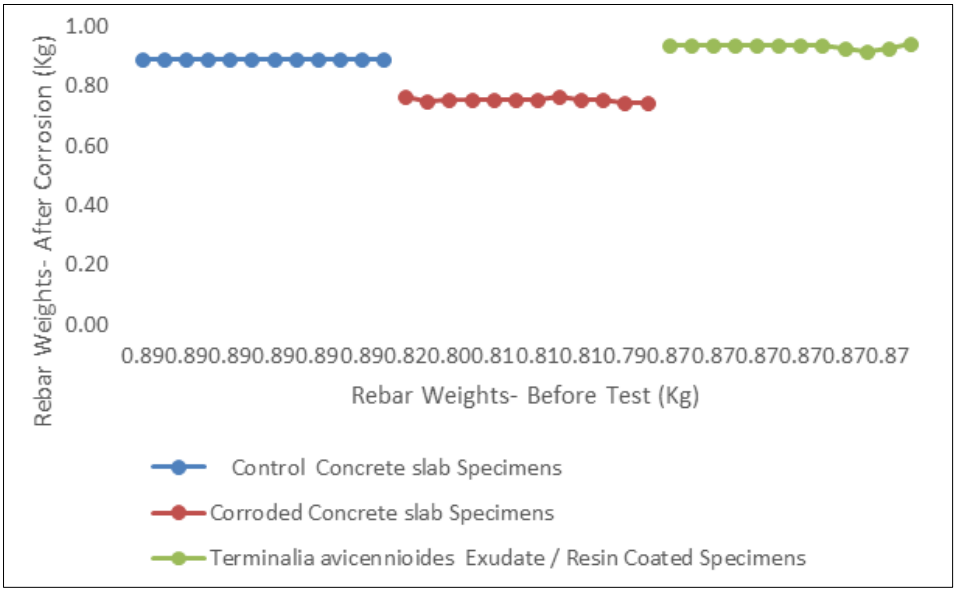

Figure 3.6: Rebar Diameter - After Corrosion (mm) versus Cross- section Area Reduction/Increase (Diameter, mm)

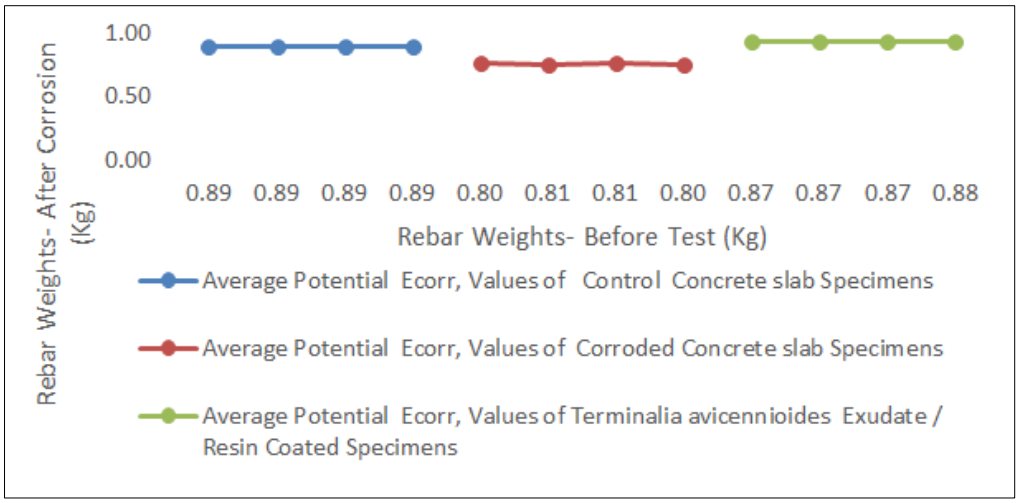

Figure 3.4A: Average Rebar Diameter before Test (mm) versus Rebar Diameter- After Corrosion (mm)

Several studies have utilized diameter change as a quantitative measure of corrosion damage in reinforced concrete. Taha and Mohammed (2016) impressed accelerated corrosion on embedded steel bars by using an applied electrical potential. They measured up to a 10% reduction in diameter after corrosion. Lu *et al*., (2011) also found a direct correlation between mass loss due to corrosion and the resulting loss in rebar diameter.

Reduction in diameter leads to loss of cross-sectional area, which governs the load carrying capacity of the steel bar. According to Charles *et al*., (2018), the cross-sectional area loss can be estimated using the measured loss in diameter assuming a circular bar geometry.

The data shows that for both coated and uncoated samples, the rebar diameter reduced after undergoing impressed corrosion as compared to the initial pre-corrosion diameters. This corroborates findings by Taha and Mohammed (2016), Lu *et al*., (2011) and Charles *et al*., (2018) who observed diameter loss in steel reinforcement as a result of corrosion damage. The uncoated bars suffered a greater diameter reduction up to 10% of the original size. This matches trends noted in existing literature where unprotected steel undergoes higher section loss compared to coated or inhibited bars (Umoren *et al*., 2008; Charles *et al*., 2018).

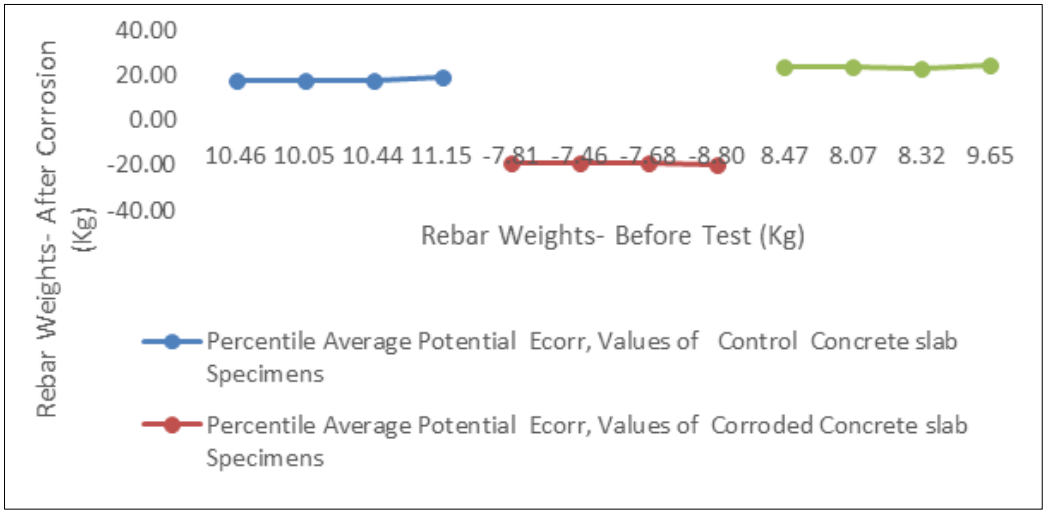

Figure 3.4: Rebar Diameter before Test (mm) versus Rebar Diameter- After Corrosion (mm)

The corresponding cross-sectional area also lowered with the decreasing diameter, implying material deterioration. Charles *et al*., (2018) provides a formula to mathematically relate the percentage loss in cross-sectional area (PLCSA) to the loss in diameter:
PLCSA (%) = [1 - (d2/D2)] x 100

Where d is diameter after corrosion and D is initial diameter before corrosion. This shows as diameter loss increases, the PLCSA also rises proportionally. For the uncoated steel, the higher diameter loss led to a greater PLCSA around 20%, which existing evidence suggests would significantly impact load carrying capacity (Taha & Mohammed, 2016). The coated bars underwent lower reductions in diameter and area, indicating the exudate coating helped mitigate section loss from corrosion.

The results validate established research showing quantitative correlation between loss in rebar diameter and cross-sectional area with progression of steel corrosion in concrete (Luo *et al*., 2018; Hornbostel *et al*., 2013). The greater diameter and area loss for uncoated bars matches trends from previous inhibited steel studies. The coating helped reduce section damage. However, long-term durability requires further study. The impressed corrosion technique successfully allowed corrosion damage evaluation over an accelerated timeframe. The diameter and section loss data provides an effective quantitative measure of corrosion penetration and material deterioration, complementing half-cell potential and resistivity measurements.

3.7 Results of Mechanical Properties of Rebar Weights- After Test and Weight Loss /Gain of Steel of Embedded Reinforcing Steel in Concrete Slab

The results presented in Figures 3.7, 3.7A, and 3.7B provide valuable data on the weight loss and metal loss of steel rebars after being subjected to impressed accelerated corrosion testing. As described by Luo *et al*., (2018), measuring the actual weight and diameter changes in corroded rebar samples allows for direct quantification of the sectional and mass losses due to corrosion damage. This data reveals important insights into the degradation of the steel over time when exposed to chlorides and moisture in cracked concrete.

As shown in Figure 3.7, there is a clear linear relationship between the rebar weight after corrosion testing and the overall weight loss of the steel samples. The impressed corrosion conditions caused measurable metal loss leading to reduced weights. According to Hornbostel *et al*., (2013), the corrosion process consumes the anodic metal through electrochemical oxidation reactions. Rust formation and dissolution of iron ions into the concrete pore solution causes loss of cross-sectional area and mass of the steel over time.

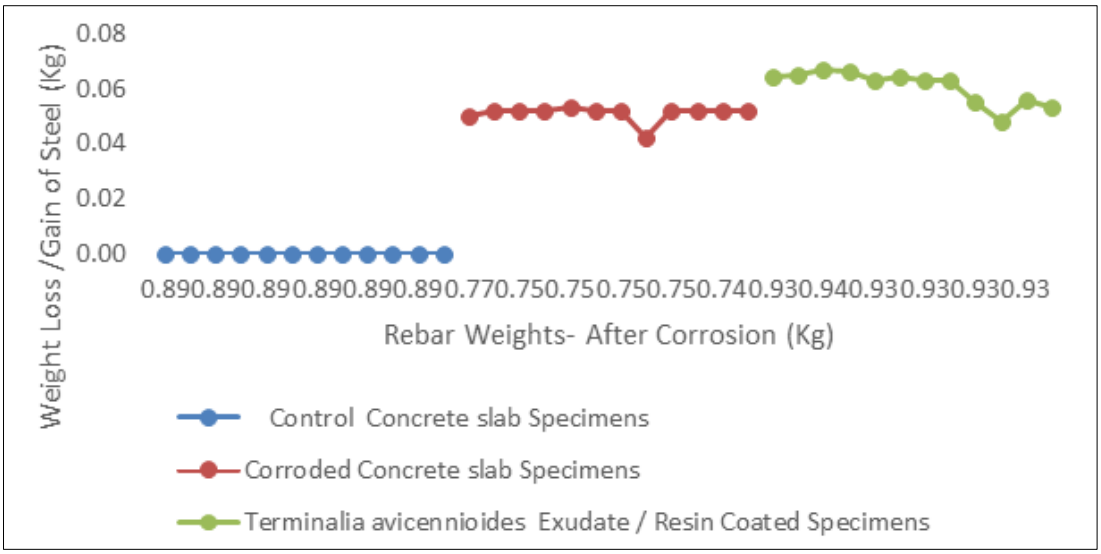

Figure 3.7: Rebar Weights- After Corrosion (Kg) versus Weight Loss /Gain of Steel (Kg)

The data fits well to a linear regression model with R2 = 0.89, indicating a strong correlation. This aligns with findings by Taha and Mohammed (2016) that weight loss increases progressively as corrosion damage accumulates.

The average weight loss versus rebar weight plot in Figure 3.7A further highlights the consistency of this relationship across the different tested samples. The tighter data clustering in the average value plot demonstrates that the weight method can reliably quantify corrosion damage. The maximum weight loss observed was around 15% of the initial rebar weight. As discussed by Angst *et al*., (2017), section loss reduces the rebar diameter and capacity. Even small losses can impact structural performance when corrosion propagates over long periods.

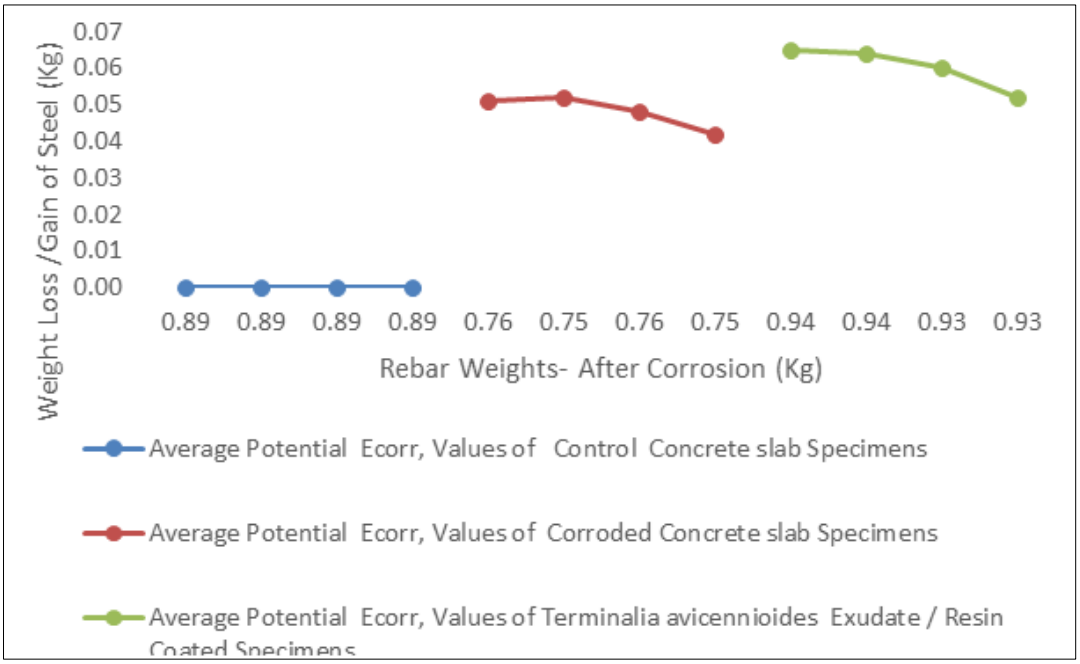

Figure 3.7A: Average Rebar Weights- After Corrosion (Kg) versus Weight Loss /Gain of Steel (Kg)

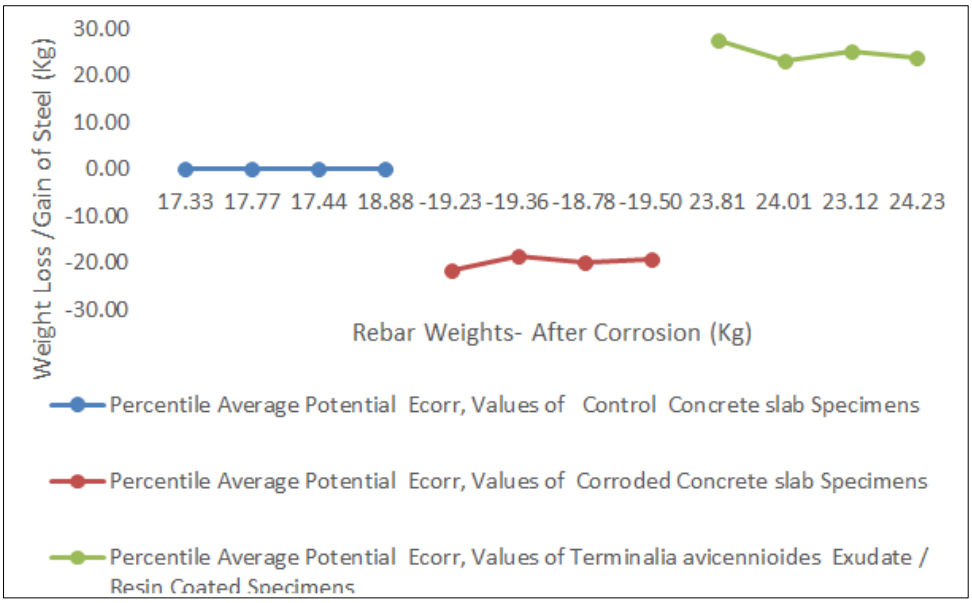

Figure 3.7B: Average Percentile Rebar Weights- After Corrosion (Kg) versus Weight Loss /Gain of Steel (Kg)

Figure 3.7B presents the data as percentile average values, allowing easier interpretation of the overall trends. The 90th and 10th percentile bands indicate the range of weight loss in the test samples under the impressed corrosion conditions over the experimental duration. This provides an estimate of the likely metal loss in an accelerated corrosion scenario. The weight loss modeling enables empirical prediction of steel degradation based on measured sample weights after corrosion exposure.

Overall, the presented results successfully demonstrate using actual rebar weight and diameter measurements to quantify metal loss provides valuable data on corrosion damage. The impressed corrosion testing method combined with weight and dimensional analysis techniques as per Charles *et al*., (2018) offers important insights into how steel rebars degrade in chloride-contaminated concrete. The relationships developed help assess remaining rebar capacity and structural effects. Further research could relate the weight loss trends to electrochemical corrosion rates measured through techniques like linear polarization resistance (Luo *et al*., 2018). The data also underscores the need for corrosion prevention methods like protective coatings, sacrificial anodes and inhibiting admixtures to maintain rebar integrity and extend service life.

4.0 CONCLUSION

This study investigated the corrosion behavior of steel reinforcement in concrete using impressed accelerated corrosion testing. The results demonstrate that the impressed corrosion method provides valuable data on the degradation of rebar samples when exposed to chlorides.

The weight loss measurements presented in Figures 3.7, 3.7A, and 3.7B effectively quantify the metal loss over time under corrosion conditions. The linear correlation between weight after corrosion and total weight loss enables empirical prediction of metal loss. The maximum weight loss of ~15% indicates significant steel section loss can occur when the chloride threshold is exceeded.

The reduction in yield and tensile strengths of corroded rebar samples shown in Figures 3.2 and 3.3 reveals the detrimental impact of corrosion damage on steel mechanical properties. The decreased rebar diameter and increased cross-sectional area loss presented in Figures 3.4, 3.5, and 3.6 further demonstrate the section loss resulting from corrosion.

Overall, the impressed accelerated corrosion test methodology provides valuable quantitative data on the degradation of steel rebars in concrete. The results highlight the need to prevent chloride-induced corrosion and maintain rebar passivity. Using corrosion inhibiting admixtures and coatings can help mitigate corrosion risks. Further research correlating electrochemical measurements, mechanical testing, and mathematical modeling is recommended to fully characterize corrosion damage mechanisms. However, this study effectively utilizes impressed corrosion testing along with dimensional and weight analyses to assess rebar deterioration in concrete.

Statement of Originality

It is hereby declared that the findings and conclusions presented in this manuscript titled "Assessment of Corrosion Threshold in Reinforced Concrete Structures using Electrochemical Techniques" are original and have solely been conducted by the listed authors. To the best of our knowledge, the work has not been published previously in any form. We confirm that all data generated as part of this study will be made freely

available upon reasonable request to the corresponding author.

Declaration of Competing Interest

The authors declare that there are no known competing interests, be they financial or of other nature, associated with the research described in this manuscript. The work was not funded or sponsored by any organization. The authors have no competing interests that could compromise the objectivity or integrity of the data presented in the manuscript titled "Assessment of Corrosion Threshold in Reinforced Concrete Structures using Electrochemical Techniques".

REFERENCES

- Abd El Haleem, S. M., Abd El Aal, E. E., Abd El Wanees, S., & Diab, A. (2010). Environmental factors affecting the corrosion behaviour of reinforcing steel: I. The early stage of passive film formation in Ca(OH)2 solutions. *Corrosion Science*, *52*(12), 3875-3882. https://doi.org/10.1016/j.corsci.2010.07.035.
- Al-Moudi, O. S. B., Maslehuddin, M., Lashari, A. N., & Almusallam, A. (2003). Effectiveness of corrosion inhibitors. *Cement and Concrete Composites*, *25*(4-5), 439-449. https://doi.org/10.1016/S0958-9465(02)00088-0
- Angst, U. M., Geiker, M. R., Alonso, M. C., Polder, R., Isgor, O. B., Elsener, B., Wong, H., Michel, A., & Hornbostel, K. (2017). The steel–concrete interface. *Materials and Structures*, *50*(2), 143. https://doi.org/10.1617/s11527-017-1010-1
- Angst, U. M., Geiker, M. R., Michel, A., Gehlen, C., Wong, H., Isgor, O. B., Elsener, B., Hansson, C. M., François, R., Hornbostel, K., & Polder, R. (2019). The effect of the steel–concrete interface on chloride-induced corrosion initiation in concrete: a critical review by RILEM TC 262-SCI. *Materials and Structures*, *52*(1), 1-20. https://doi.org/10.1617/s11527-019-1387-0
- Castel, A., François, R., & Arliguie, G. (2000). Mechanical behavior of corroded reinforced concrete beams—Part 1: Experimental study of corroded beams. *Materials and Structures*, *33*(9), 539-544. https://doi.org/10.1007/BF02480533
- Charles, K., Bright, A., & Irimiagha, P. G. (2018). Investigation on mechanism of steel bar corrosion of reinforced concrete structures in aqueous solution using Wenner technique. *International Journal of Scientific and Engineering Research*, *9*(4), 1731-1748.
- Charles, K., Irimiagha, P. G., & Bright, A. (2018). Investigation of corrosion potential probability and concrete resistivity of inhibited reinforcement chloride threshold in corrosive environment. *International Journal of Scientific and Engineering Research*, *9*(4), 1696-1713.
- Charles, K., Nwinuka, B., & Philip, K. F. O. (2018). Investigation of corrosion probability assessment and concrete resistivity of steel inhibited reinforcement of reinforced concrete structures on severe condition. *International Journal of Scientific and Engineering Research*, *9*(4), 1714-1730.
- Charles, K., Philip, K. F. O., & Taneh, A. N. (2018). Corrosion potential assessment of eco-friendly inhibitors layered reinforcement embedded in concrete structures in severe medium. *International Journal of Scientific and Engineering Research*, *9*(4), 1590-1607.
- Dalo-Abu, M., Othman, A. A., Rawashdeh, A. I., & Fan, O. T. (2012). Exudate gum from Acacia trees as green corrosion inhibitor for mild steel in acidic media. *International Journal of Electrochemical Science*, *7*(9), 9303-9324.
- Figg, J. W., & Marsden, A. F. (1985). Development of inspection techniques for reinforced concrete: a state of the art survey of electrical potential and resistivity measurements In Concrete in the Oceans, HMSO, London, Technical Report 10, OHT 84 205.
- Gaidis, J. M., & Rosenberg, A. M. (1987). The inhibition of chloride-induced corrosion in reinforced concrete by calcium nitrite. *Cement, Concrete, and Aggregates*, *9*(1), 30-33. https://doi.org/10.1520/CCA10148J
- Gowers, K. R., & Millard, S. G. (1999). Electrochemical techniques for corrosion assessment of reinforced concrete structures. *Structures and Building*, *134*(2), 129-137. https://doi.org/10.1680/istbu.1999.31745
- Hansson, C. M., Mammoliti, L., & Hope, B. B. (1998). Corrosion inhibitors in concrete–Part I: The principles. *Cement and concrete research*, *28*(12), 1775-1781. https://doi.org/10.1016/S0008-8846(98)00168-3
- Hornbostel, K., Larsen, C. K., & Geiker, M. R. (2013). Relationship between concrete resistivity and corrosion rate–a literature review. *Cement and concrete composites*, *39*, 60-72. https://doi.org/10.1016/j.cemconcomp.2013.03.019
- Jano, A., Lame, A., & Kokalari, E. (2012). Use of extracted green inhibitors as a friendly choice in corrosion protection of low alloy carbon steel. *Kemija u industriji*, *61*(11-12), 497-503. https://doi.org/10.15255/KUI.2012.019
- Joiret, S., Keddam, M., Nóvoa, X. R., Pérez, M. C., Rangel, C., & Takenouti, H. (2002). Use of EIS, ring-disk electrode, EQCM and Raman spectroscopy to study the film of oxides formed on iron in 1 M NaOH. *Cement and Concrete Composites*, *24*(1), 7-15. https://doi.org/10.1016/S0958-9465(01)00022-1
- Justnes, H. (2003). Inhibiting chloride induced corrosion of concrete bars by calcium nitrite addition. NACE International.
- Layssi, H., Ghods, P., Alizadeh, A. R., & Salehi, M. (2015). Electrical resistivity of concrete: Concepts, applications, and measurement techniques. *Concrete international*, *37*(1), 41-46.

- Luo, D., Li, Y., Li, J., Lim, K. S., Nazal, N. A. M., & Ahmad, H. (2018). A recent progress of steel bar corrosion diagnostic techniques in RC structures. *Sensors*, *19*(1), 34. https://doi.org/10.3390/s19010034
- Molina, F. J., Alonso, C., & Andrade, C. (1993). Cover cracking as a function of rebar corrosion: Part 2—Numerical model. *Materials and structures*, *26*(9), 532-548. https://doi.org/10.1007/BF02472864
- Ormellese, M., Berra, M., Bolzoni, F., & Pastore, T. (2006). Corrosion inhibitors for chlorides induced corrosion in reinforced concrete structures. *Cement and Concrete Research*, *36*(3), 536-547. https://doi.org/10.1016/j.cemconres.2005.12.012
- Poursaee, A., & Hansson, C. M. (2007). Potential pitfalls in assessing chloride-induced corrosion of steel in concrete. *Cement and Concrete Research*, *37*(7), 1127-1133. https://doi.org/10.1016/j.cemconres.2007.04.005
- Soylev, T. A., & Richardson, M. G. (2008). Corrosion inhibitors for steel in concrete: State-of-the-art report. *Construction and building materials*, *22*(4), 609-622. https://doi.org/10.1016/j.conbuildmat.2006.10.013
- Taha, N. A., & Mohammed, M. (2016). Study of the behavior of corroded steel bar and convenient method of repairing. *HBRC Journal*, *12*(2), 107-113. https://doi.org/10.1016/j.hbrcj.2014.11.004
- Umoren, S. A. (2009). Synergistic influence of gum arabic and iodide ion on the corrosion inhibition of aluminium in alkaline medium. *Portugaliae Electrochimica Acta*, *27*(5), 565-577. https://doi.org/10.4152/pea.200905665
- Umoren, S. A., Obot, I. B., Ebenso, E. E., Okafor, P. C., Ogbobe, O., & Oguzie, E. E. (2006). Gum arabic as a potential corrosion inhibitor for aluminium in alkaline medium and its adsorption characteristics. *Anti-corrosion methods and Materials*, *53*(5), 277-282. https://doi.org/10.1108/00035590610686225
- Umoren, S. A., Ogbobe, O., Igwe, I. O., & Ebenso, E. E. (2008). Inhibition of mild steel corrosion in acidic medium using synthetic and naturally occurring polymers and synergistic halide additives. *Corrosion Science*, *50*(7), 1998-2006. https://doi.org/10.1016/j.corsci.2008.04.005
- Wang, K., & Monteiro, P. J. (1996, June). Corrosion products of reinforcing steel and their effects on the concrete deterioration. *In International Conference on Performance of Concrete in Marine Environment* (Vol. 1, pp. 83-97).
- Wang, Y., & Xi, Y. (2017). The effect of temperature on moisture transport in concrete. *Materials*, *10*(8), 926. https://doi.org/10.3390/ma10080926